SLAC-PUB-144
NOVEMBER 1965

W MESON PRODUCTION IN $\pi^- + p \rightarrow W^- + p$ INTERACTIONS*

J. D. Sullivan

Stanford Linear Accelerator Center
Stanford University, Stanford, California

ABSTRACT

The cross section for production of W bosons in the reaction $\pi^- + p \rightarrow W^- + p$ is calculated on the basis of single particle exchange for W masses in the region 2-5 BeV. Corrections for absorption in the initial channel are included. Pion exchange is found to dominate rho exchange and gives $(4 - 12) \times 10^{-34}$ cm^2 as a lower bound to the total production cross section.

(Submitted to Physical Review)

*Work supported by U. S. Atomic Energy Commission

I. INTRODUCTION

The present V-A theory of weak interactions naturally accommodates a charge 1, spin 1 particle usually called the W boson.[1] This particle is supposed to have weak and electromagnetic couplings but no strong couplings. There is no theoretical prediction of the W boson mass, but recent high energy neutrino experiments[2] have set 1.3 – 1.8 BeV as a lower limit.

In the search for this elusive particle no possible production mechanism should be overlooked. Consequently we present here calculations of the expected production cross sections of W^- mesons in the reaction $\pi^- + p \rightarrow W^- + p$. We use the peripheral model, including initial state absorption corrections, and consider both pseudoscalar and vector exchange; Fig. 1. Basically our model is a generalization and extension to higher energies of that of Bernstein and Feinberg.[3]

The W meson, if it exists, would be highly unstable and would be detectable only through observation of its decay products. Detection in the reaction $\pi^- + p \rightarrow W^- + p$ would be a formidable experimental problem because of the large backgrounds that would be present. Except for a few remarks in the conclusion we will not attempt to discuss what kinematical and dynamical features might be used to distinguish true W events from background. Our purpose here is to provide realistic estimates of W meson production cross sections which can be used in any serious discussion.

In Section II we discuss the W couplings we require and in Section III the particular form of the absorption corrections we employ. In Sections IV and V we present the calculations and results for π and ρ exchange, respectively. Section VI contains our concluding remarks.

II. W MESON COUPLINGS

In our notation the weak Hamiltonian describing the coupling of W mesons is

$$H_W = g_W\left(J^H_\alpha(x) + J^L_\alpha(x)\right) W^{(+)\alpha}(x) + g_W\left(J^H_\alpha(x) + J^L_\alpha(x)\right)^\dagger W^{(-)\alpha}(x) \qquad (2.1)$$

where

$$J^L_\alpha = \bar{\nu}_\mu \gamma_\alpha(1 - \gamma_5)\,\mu^- + \bar{\nu}_e \gamma_\alpha(1 - \gamma_5)\, e^- \qquad (2.2)$$

is the leptonic weak current and

$$J^H_\alpha = V_\alpha + A_\alpha \qquad (2.3)$$

is the hadron weak current with vector (V_α) and axial vector (A_α) parts. In Eqs. (2.1) and (2.2) the particle symbols stand for the corresponding field operators. The constant g_W is given by

$$g_W^2 = m_W^2\, G/\sqrt{2} \qquad (2.4)$$

where G is the Fermi coupling constant ($Gm_N^2 \cong 10^{-5}$). Little is known about J^H_α except general properties implied by Lorentz invariance and group theoretic transformation properties. A few of its matrix elements between simple states are known from experiment. In particular to calculate the diagrams of Figs. 1(a) and 1(b), we require $< \pi^o;\, q_2 \left| J^H_\alpha \right| \pi^-;\, q_1 >$ and $< \rho^o;\, q_2 \left| J^H_\alpha \right| \pi^-;\, q_1 >$. We neglect all form factors so that we merely seek the values of the $\pi\pi W$ and $\rho\pi W$ coupling constants. For $< \pi^o;\, q_2 \left| J^H_\alpha \right| \pi^-;\, q_1 >$ only the vector part V_α contributes and has a value fixed by the conserved vector current hypothesis[3,4] (CVC)

$$\sqrt{2q_1^o\, 2q_2^o}\; < \pi^o;\, q_2 \left| V_\alpha(o) \right| \pi^-;\, q_1 > = \sqrt{2}\,(q_1 + q_2)_\alpha \,. \qquad (2.5)$$

For $< \rho^o; q_2 \left| J_\alpha^H \right| \pi^- ; q_1 >$ only the axial vector part A_α makes a contribution. This follows from the observation that the ρ and π have opposite G parity and so are coupled only by odd G parity operators like A_α.[5] To determine the strength of the coupling we make use of the partially conserved axial vector current hypothesis (PCAC) in a manner analogous to the most popular derivation[6] of the Goldberger-Treiman relation.[7] The partial conservation hypothesis is the statement that the matrix elements of $\partial^\alpha A_\alpha$ vanish in the limit of infinite momentum transfer. This argument has already been presented in detail by Beg, Cornwall and Woo,[8] for the $\rho\pi$ matrix element, but we briefly resketch the derivation in order to fix our notation. We have from the diagrams of Fig. 2(a) and Fig. 2(b)

$$\sqrt{2q_1^o\, 2q_2^o} < \rho^o; q_2 \left| A_\alpha(0) \right| \pi^- ; q_1 > = - b_{\rho\pi} \epsilon_\alpha(q_2) + a_\pi g_{\rho\pi\pi} \frac{2\epsilon(q_2) \cdot q_1 (q_1 - q_2)_\alpha}{(q_1 - q_2)^2 - \mu^2} \qquad (2.6)$$

where ϵ is the ρ polarization vector, a_π the pion-W meson coupling constant, $b_{\rho\pi}$ the phenomenological direct $\rho\pi W$ coupling that we seek, and $g_{\rho\pi\pi}$ the $\rho\pi\pi$ coupling constant which is given in terms of the ρ width $\Gamma_{\rho\pi\pi}$ by

$$\frac{g_{\rho\pi\pi}^2}{4\pi} = \frac{6m_\rho^2}{(m_\rho^2 - 4m_\pi^2)^{3/2}} \Gamma_{\rho\pi\pi} \ . \qquad (2.7)$$

From Eq. (2.6) we have that

$$\sqrt{2q_1^o\, 2q_2^o} < \rho^o; q_2 \left| \partial^\alpha A_\alpha(0) \right| \pi^- ; q_1 > = ib_{\rho\pi} \epsilon \cdot q_1 - ia_\pi g_{\rho\pi\pi} \frac{2\epsilon \cdot q_1 (q_1 - q_2)^2}{(q_1 - q_2)^2 - \mu^2} \ . \qquad (2.8)$$

Requiring this to vanish as $(q_1 - q_2)^2 \to \infty$ fixes

$$b_{\rho\pi} = 2a_\pi g_{\rho\pi\pi} \quad . \tag{2.9}$$

The continuum contributions [Fig. 2(c)], which we have not included in Eq. (2.8), separately vanish in this limit and consequently do not effect Eq. (2.9). Substituting for a_π the Goldberger-Treiman relation[7]

$$a_\pi = \frac{-\sqrt{2}\, m_N \alpha}{g_{\pi NN}} \tag{2.10}$$

where $\alpha = G_A/G_V \cong -1.18$ and $g_{\pi NN}$ is the pion-nucleon coupling constant as usually defined, we have

$$b_{\rho\pi} = \frac{-2\sqrt{2}\, g_{\rho\pi\pi}\, m_N \alpha}{g_{\pi NN}} \quad . \tag{2.11}$$

Numerically we find $\left| b_{\rho\pi} \right| = 1.23\, m_N$.

III. ABSORPTION CORRECTIONS

We discuss in this section the corrections we apply to the Born diagrams of Fig. 1. The particular form we employ is that used by Gottfried and Jackson[9] and others[10] to successfully fit (especially for pseudoscalar exchange) a great number of production reactions in the 2 – 8 BeV region.

In this scheme the corrected partial wave helicity amplitudes $F^j_{\lambda_3\lambda_4;\lambda_1\lambda_2}(s)$ are given in terms of the Born approximation partial wave helicity amplitudes $F^{Bj}_{\lambda_3\lambda_4;\lambda_1\lambda_2}(s)$ by

$$F^j_{\lambda_3\lambda_4;\lambda_1\lambda_2}(s) = e^{i\delta^j_F(s)}\, F^{Bj}_{\lambda_3\lambda_4;\lambda_1\lambda_2}(s)\, e^{i\delta^j_I(s)} \tag{3.1}$$

where $\delta_I^j(s)$ and $\delta_F^j(s)$ are the elastic scattering phase shifts for angular momentum j in the initial and final states respectively. In Eq. (3.1) the usual simplifying approximation has been made that the elastic scattering is a scalar in the helicity indices. In the limit that the elastic scattering phase shifts are pure imaginary[11] we may write Eq. (3.1) as

$$F^j_{\lambda_3\lambda_4;\lambda_1\lambda_2}(s) = \sqrt{\eta_F^j}\, F^{Bj}_{\lambda_3\lambda_4;\lambda_1\lambda_2}\, \sqrt{\eta_I^j} \tag{3.2}$$

where the inelasticity parameters

$$\eta^j_{I,F} = \left| e^{2i\delta^j_{I,F}} \right| \tag{3.3}$$

may be obtained from the shape of the elastic scattering peaks of the initial and final channels.

In the reaction considered here $\eta_j^F = 1$, since there are no final state interactions, and η_j^I is to be determined from $\pi^- p$ scattering data. If we parameterize the $\pi^- p$ diffraction peak as

$$f(s,t) = f(s,o)\, e^{\frac{1}{2}A(s)t} = \frac{iq}{4\pi}\, \sigma_{tot}(s)\, e^{\frac{1}{2}A(s)t} \tag{3.4}$$

then

$$\eta^j(s) = 1 - \frac{q^2}{4\pi}\, \sigma_{tot}\, \frac{1}{2} \int_{-1}^{+1} dz P_\ell(z)\, e^{\frac{1}{2}A(s)t} \tag{3.5}$$

where: $t = -2q^2(1-z)$ and $j = \ell + 1/2$. In our work we have further simplified Eq. (3.5) to the "impact parameter" result[9]

$$\eta^j(s) = 1 - \frac{\sigma_{tot}}{4\pi A} \exp\left(\frac{-(j-\frac{1}{2})^2}{2Aq^2}\right). \tag{3.6}$$

The particular values of A and σ_{tot} that we use are[12] $A = 9.4(\text{BeV})^{-2}$ independent of s, corresponding to a non-shrinking diffraction peak, and[13] $\sigma_{tot} \cong 27$ mb. In view of the fact that most absorption model fits are best when the S-wave ($j = 1/2$) is fully absorbed, we also show the effect on our results of setting $\sigma_{tot}/4\pi A = 1$. This latter choice should assure a lower bound for the cross section.

IV. W PRODUCTION BY PION EXCHANGE

The S matrix element for the diagram of Fig. 1(a) is

$$S = \sqrt{\frac{m_N^2}{4q_o k_o E_1 E_2}}\,(2\pi)^4\,\delta^4(k + p_2 - q - p_1)\,2\sqrt{2}\,g_W g_{\pi NN}\,\frac{1}{4m_N\sqrt{(E_1+m)(E_2+m)}}\,F \qquad (4.1)$$

where

$$F = 4m_N\sqrt{(E_1+m)(E_2+m)}\,\frac{\bar{u}(p_2)\,\gamma_5\,u(p_1)}{t - m_\pi^2}\,q\cdot\epsilon^* \quad , \qquad (4.2)$$

ϵ is the W polarization vector, $t = (k-q)^2$, and q_o, k_o, E_1, E_2 are the center-of-mass energies of the incident pion, the W meson, the initial proton and the final proton, respectively. The center-of-mass differential cross section for unpolarized particles is given by

$$\left(\frac{d\sigma}{d\Omega}\right)_{cm} = \frac{1}{8\pi}\left(\frac{g_{\pi NN}^2}{4\pi}\right) g_W^2\,\frac{p_2}{p_1 s(E_1+m)(E_2+m)}\,\frac{1}{2}\sum_{\text{spins}}|F|^2 \qquad (4.3)$$

where $s = (p_1 + q)^2$. Neglecting initial state absorption gives as an upper limit to the cross section

$$\left(\frac{d\sigma}{d\Omega}\right)_{cm}^{\text{No. Abs.}} = \frac{1}{8\pi}\left(\frac{g_{\pi NN}^2}{4\pi}\right)\left(\frac{g_W^2}{m_W^2}\right)\frac{p_2}{p_1 s}\,\frac{(-t)\left[t - (m_W+m_\pi)^2\right]\left[t - (m_W-m_\pi)^2\right]}{(t - m_\pi^2)^2} \quad . \qquad (4.4)$$

Using $g^2_{\pi NN}/4\pi = 14.6$, Eq. (2.4) and integrating Eq. (4.4) we obtain for the total cross section without absorption the results given in Table I for $m_W = 2, 3, 4, 5$ at selected incident pion lab energies (denoted by ν).

To analyze the effect of the initial state interactions we project out the six independent helicity amplitudes $F_{\lambda,\lambda_2;\lambda'\lambda_1}$ from Eq. (4.2). Here $\lambda,\lambda_2;\lambda',\lambda_1$ denote the helicities of the outgoing W, the final proton, the incident pion and the initial proton respectively.

$$F_1 = F_{1\frac{1}{2}:0\frac{1}{2}} = -\frac{p_1(\epsilon_1 - \epsilon_2)}{\sqrt{2}} \frac{\sin\theta\cos\theta/2}{\beta-\cos\theta}$$

$$F_2 = F_{1\frac{1}{2}:0-\frac{1}{2}} = \frac{p_1(\epsilon_1 + \epsilon_2)}{\sqrt{2}} \frac{\sin\theta\sin\theta/2}{\beta-\cos\theta}$$

$$F_3 = F_{0\frac{1}{2}:0\frac{1}{2}} = (\epsilon_1 - \epsilon_2)\left(\frac{q_o p_2 - k_o p_1\cos\theta}{m_W}\right)\frac{\cos\theta/2}{\beta-\cos\theta} \qquad (4.5)$$

$$F_4 = F_{0\frac{1}{2}:0-\frac{1}{2}} = -(\epsilon_1 + \epsilon_2)\left(\frac{q_o p_2 - k_o p_1\cos\theta}{m_W}\right)\frac{\sin\theta/2}{\beta-\cos\theta}$$

$$F_5 = F_{1-\frac{1}{2}:0\frac{1}{2}} = F_2$$

$$F_6 = F_{1-\frac{1}{2}:0-\frac{1}{2}} = -F_1$$

where
$$\epsilon_1 = \frac{E_1 + m}{p_1}, \quad \epsilon_2 = \frac{E_2 + m}{p_2}, \quad \beta = \frac{2E_1E_2 + m_\pi^2 - 2m_N^2}{2p_1p_2}, \qquad (4.6)$$

and θ is the W production angle in the center-of-mass. The remaining six helicity amplitudes which have not been listed are related to Eq. (4.5) by parity invariance according to

$$F_{\lambda\lambda_2:0\lambda_1} = -(-1)^{\lambda-\lambda_2+\lambda_1} F_{-\lambda-\lambda_2;0-\lambda_1}. \qquad (4.7)$$

The equalities $F_5 = F_2$ and $F_6 = -F_1$ are special to the Born approximation and are removed when the absorption corrections are included.

The partial wave projections for Eq. (4.5) are obtained from

$$F^j_{\lambda\lambda_2;\lambda'\lambda_1} = \frac{1}{2}\int_{-1}^{+1} d\cos(\theta)\, d^j_{\lambda'-\lambda;\lambda-\lambda_2}(\theta)\, F_{\lambda\lambda_2;\lambda'\lambda_1}(\theta) \tag{4.8}$$

and the required d functions are:

$$\begin{aligned}
d^j_{-\frac{1}{2}\frac{1}{2}}(\theta) &= -\, d^j_{\frac{1}{2}-\frac{1}{2}}(\theta) = \frac{\sin\theta/2}{\ell+1}\left\{P'_{\ell+1} + P'_\ell\right\} \\
d^j_{\frac{1}{2}\frac{1}{2}}(\theta) &= d^j_{-\frac{1}{2}-\frac{1}{2}}(\theta) = \frac{\cos\theta/2}{\ell+1}\left\{P'_{\ell+1} - P'_\ell\right\} \\
d^j_{-\frac{1}{2}\frac{3}{2}}(\theta) &= \frac{\cos\theta/2}{(\ell+1)\sqrt{\ell(\ell+2)}}\left\{-\ell P'_{\ell+1} + (\ell+2)\,P'_\ell\right\} \\
d^j_{\frac{1}{2}\frac{3}{2}}(\theta) &= \frac{\sin\theta/2}{(\ell+1)\sqrt{\ell(\ell+2)}}\left\{\ell P'_{\ell+1} + (\ell+2)\,P'_\ell\right\}
\end{aligned} \tag{4.9}$$

where $\ell = j-\frac{1}{2}$. Carrying out the angular projections for the amplitudes Eq. (4.5) yields:

$$\begin{aligned}
(2j+1)\,F^j_1 &= \frac{p_1(\epsilon_1-\epsilon_2)}{\sqrt{2}}\left\{(\ell+1)(1+\beta)(Q_{\ell+1}-Q_\ell) + \delta_{\ell 0}\right\} \\
(2j+1)\,F^j_2 &= \frac{p_1(\epsilon_1+\epsilon_2)}{\sqrt{2}}\left\{(\ell+1)(1-\beta)(Q_{\ell+1}+Q_\ell) + \delta_{\ell 0}\right\} \\
(2j+1)\,F^j_3 &= \frac{(\epsilon_1-\epsilon_2)}{m_W}\left\{(q_o p_2 - k_o p_1\beta)(\ell+1)(Q_{\ell+1}+Q_\ell) + k_o p_1\,\delta_{\ell 0}\right\} \\
(2j+1)\,F^j_4 &= -\left(\frac{\epsilon_1+\epsilon_2}{m_W}\right)\left\{q_o p_2 - k_o p_1\beta)(\ell+1)(Q_{\ell+1}-Q_\ell) - k_o p_1\,\delta_{\ell 0}\right\} \\
(2j+1)\,F^j_5 &= \frac{-p_1(\epsilon_1+\epsilon_2)}{\sqrt{2\ell(\ell+1)}}(1-\beta^2)\left(\ell Q'_{\ell+1} - (\ell+2)Q'_\ell\right) \qquad \ell \neq 0 \\
(2j+1)\,F^j_6 &= \frac{p_1(\epsilon_1-\epsilon_2)}{\sqrt{2\ell(\ell+1)}}(1-\beta^2)\left(\ell Q'_{\ell+1} + (\ell+2)\,Q'_\ell\right) \qquad \ell \neq 0\,.
\end{aligned} \tag{4.10}$$

Finally, the full helicity amplitudes for pion exchange corrected for initial state absorption are:

$$
\begin{aligned}
F_1 &= \sum_{j=\frac{1}{2}}^{\infty} (2j+1)\, F_1^j \sqrt{\eta^j}\, d^j_{-\frac{1}{2}\frac{1}{2}}(\theta) \\
F_2 &= \sum_{j=\frac{1}{2}}^{\infty} (2j+1)\, F_2^j \sqrt{\eta^j}\, d^j_{\frac{1}{2}\frac{1}{2}}(\theta) \\
F_3 &= \sum_{j=\frac{1}{2}}^{\infty} (2j+1)\, F_3^j \sqrt{\eta^j}\, d^j_{-\frac{1}{2}-\frac{1}{2}}(\theta) \\
F_4 &= \sum_{j=\frac{1}{2}}^{\infty} (2j+1)\, F_4^j \sqrt{\eta^j}\, d^j_{\frac{1}{2}-\frac{1}{2}}(\theta) \\
F_5 &= \sum_{j=\frac{3}{2}}^{\infty} (2j+1)\, F_5^j \sqrt{\eta^j}\, d^j_{-\frac{1}{2}\frac{3}{2}}(\theta) \\
F_6 &= \sum_{j=\frac{3}{2}}^{\infty} (2j+1)\, F_6^j \sqrt{\eta^j}\, d^j_{\frac{1}{2}\frac{3}{2}}(\theta) \ .
\end{aligned}
\tag{4.11}
$$

Determining the η^j's as described in Section III and using Eqs. (2.4), (4.3) and (4.11) we find the center-of-mass differential cross sections plotted in Figs. 3, 4, 5 and 6. We have also plotted there the cross sections, Eq. (4.4), before absorption corrections. In Fig. 7 we display for the case $m_W = 3$ BeV, $\nu = 16$ BeV, $\sigma_{tot}/4\pi A = 1$, the behavior of the cross section as the $j = 1/2, 3/2, 5/2$, etc. partial waves are successively corrected for absorption. Table I lists also the total cross sections obtained from these curves.

V. W PRODUCTION BY RHO EXCHANGE

The rho exchange diagram of Fig. 1(b) gives the S matrix element

$$S = \sqrt{\frac{m_N^2}{4q_o k_o E_1 E_2}}\,(2\pi)^4\,\delta^4(k + p_2 - q - p_1)\,\frac{g_W\, b_{\rho\pi}\, g_{\rho NN}}{2}\,\frac{1}{4m_N\sqrt{(E_1+m)(E_2+m)}}\,F \qquad (5.1)$$

where

$$F = 4m_N\,\sqrt{(E_1+m)(E_2+m)}\,\frac{\bar{u}(p_2)\,\gamma_\mu\,u(p_1)\,\epsilon^{\mu *}}{t - m_\rho^2} \qquad (5.2)$$

and all other variables are the same as in Section IV. The center-of-mass differential cross section is given by Eq. (4.3) except that $g_{\pi NN}^2/4\pi$ in that expression is to be replaced by $(g_{\rho NN}^2/4\pi)(b_{\rho\pi}^2/32)$. Neglecting initial state absorption, Eqs. (5.1) and (5.2) give for unpolarized particles

$$\left(\frac{d\sigma}{d\Omega}\right)_{cm}^{\text{No Abs.}} = \left(\frac{g_{\rho NN}^2}{4\pi}\right)\left(\frac{b_{\rho\pi}^2}{64\pi}\right)\left(\frac{g_W^2}{m_W^2}\right)\frac{p_2}{p_1^s}\,\frac{\left[(s - m_N^2 - m_W^2)(t + s - m_N^2 - m_\pi^2) - m_W^2(t + 4m_N^2)\right]}{(t - m_\rho^2)^2}\,. \qquad (5.3)$$

We use Eq. (2.11) for $b_{\rho\pi}$ and assume that the ρ meson is universally coupled to the isospin current to obtain $g_{\rho NN} = g_{\rho\pi\pi}$. With these values of the coupling constants Eq. (5.3) gives the total cross sections listed in Table II. We have listed only a few cases since the resulting cross sections are characteristically more than an order of magnitude smaller than for pion exchange.

Again to calculate the initial state absorption corrections we project from Eq. (5.2) the six independent helicity amplitudes. In the notation

of Section IV these are:

$$F_1 = -\sqrt{2}\,(\epsilon_1 + \epsilon_2)\,\frac{\sin\theta/2}{\gamma-\cos\theta}$$

$$F_2 = -\sqrt{2}\,(\epsilon_1 - \epsilon_2)\,\frac{\cos\theta/2}{\gamma-\cos\theta}$$

$$F_3 = -\left(\frac{p_2(1+\epsilon_1\epsilon_2) + k_o(\epsilon_1+\epsilon_2)}{m_W}\right)\frac{\cos\theta/2}{\gamma-\cos\theta} \qquad (5.4)$$

$$F_4 = -\left(\frac{p_2(1-\epsilon_1\epsilon_2) - k_o(\epsilon_1-\epsilon_2)}{m_W}\right)\frac{\sin\theta/2}{\gamma-\cos\theta}$$

$$F_5 \equiv 0$$

$$F_6 \equiv 0$$

where

$$\gamma = \frac{2E_1E_2 + m_\rho^2 - 2m_N^2}{2p_1p_2}\,. \qquad (5.5)$$

The remaining six helicity amplitudes may be obtained from

$$F_{\lambda\lambda_2;0\lambda_1} = +(-1)^{\lambda-\lambda_2+\lambda_1}\,F_{-\lambda-\lambda_2;0-\lambda_1}\,. \qquad (5.6)$$

The difference in overall sign between Eqs. (5.6) and (4.7) is due to the fact that in pion exchange the W is produced as a 1^- meson and in rho exchange as a 1^+ meson. Of course in its subsequent decay the W forgets this information.

The fact that F_3 has the same angular dependence as F_2 is a particular property of the Born approximation. However, because their partial

wave expansions have the same form [see Eq. (4.11)] this peculiar degeneracy is preserved even after absorption corrections. A similar statement applies to F_4 and F_1. Furthermore, the vanishing of F_5 and F_6 is also special to the Born approximation and is, of course, preserved by our absorption corrections. This means we need only work with F_1 and F_2 in doing the absorption calculations. Using Eqs. (4.8) and (5.4) we find for the partial wave projections:

$$\begin{aligned}(2j+1)\,F_1^j &= \sqrt{2}\,(\epsilon_1+\epsilon_2)(\ell+1)\left(Q_{\ell+1}(\gamma)-Q_\ell(\gamma)\right)\\ (2y+1)\,F_2^j &= -\sqrt{2}\,(\epsilon_1-\epsilon_2)(\ell+1)\left(Q_{\ell+1}(\gamma)+Q_\ell(\gamma)\right).\end{aligned} \tag{5.7}$$

Thus the full helicity amplitudes corrected for initial state absorptions are:

$$\begin{aligned}F_1 &= \sum_{j=\frac{1}{2}}^{\infty}(2j+1)\,F_1^j\,\sqrt{\eta^j}\,d^j_{-\frac{1}{2}\frac{1}{2}}(\theta)\\ F_2 &= \sum_{j=\frac{1}{2}}^{\infty}(2j+1)\,F_2^j\,\sqrt{\eta^j}\,d^j_{\frac{1}{2}\frac{1}{2}}(\theta)\\ F_3 &= \left(\frac{p_2(1+\epsilon_1\epsilon_2)+k_o(\epsilon_1+\epsilon_2)}{\sqrt{2}\,m_W(\epsilon_1-\epsilon_2)}\right)F_2\\ F_4 &= \left(\frac{p_2(1-\epsilon_1\epsilon_2)-k_o(\epsilon_1-\epsilon_2)}{\sqrt{2}\,m_W(\epsilon_1+\epsilon_2)}\right)F_1\\ F_5 &= F_6 = 0\ .\end{aligned} \tag{5.8}$$

We show in Figs. 8 and 9 the differential cross sections given by Eq. (5.8). In Table II we give the corresponding total cross sections.

VI. SUMMARY AND CONCLUSIONS

We have obtained differential and total cross sections for W^- meson production in $\pi^- + p \to W^- + p$ for both pion and rho exchange. Unless the strength of the $\rho\pi W$ coupling is substantially greater than is given by the PCAC hypothesis (Section II) pion exchange is the dominant process. We have shown that the absorption corrections may reduce the total production cross section by a factor of 20-80 for W masses in the region 2-5 BeV and pion energies 6-32 BeV. The reduction takes the usual form of a slight suppression of the forward amplitude and large damping in non-forward directions.

There are admittedly a large number of uncertainties in the results presented above. In spite of the many words written on the subject, no one has given a derivation of Eq. (3.1) valid when the absorption is very large. Furthermore, in the $\pi^- p$ amplitude the forward amplitude is far from pure imaginary,[11] and it is somewhat arbitrary to neglect the spin structure of πp scattering as in Eqs. (3.1) and (3.5). One might also entertain the possibility of t-dependent form factors at the vertices of Fig. 1. This possibility has been investigated empirically by Bander and Shaw[15] for the reaction $\pi^- + p \to \rho^- + p$ at $\nu = 4$ BeV with the conclusion that there is little need nor room for such form factors.

The largest uncertainty in our work occurs because of the sensitivity of the non-forward amplitude to the choice of the absorption parameter $\sigma_{tot}/4\pi A$. Setting it equal to 1 gives complete S-wave suppression and enhanced absorption of the higher partial waves. In the range $\nu = 6$-30 BeV, experimentally one has $\sigma_{tot}/4\pi A \cong 0.58$. Using this latter value gives total production cross sections about a factor 4-8 times larger than for the choice

$\sigma_{tot}/4\pi A = 1$. There is no real test of the absorption model on this point, so our results should be interpreted as upper and lower bounds.

A detail we have not included above is a form factor $F_\pi(m_W^2)$ at the $\pi^-\pi^0 W^-$ vertex in Fig. 1(a) as discussed by Bernstein and Feinberg.[3] (There would be a corresponding form factor in Fig. 1(b).) The CVC theory fixes $F_\pi(m_W^2)$ to be the pion electromagnetic form factor $F_\pi(k^2)$ (normalized to 1 at $k^2 = 0$) evaluated at $k^2 = m_W^2$. If there happens to be a $\pi\pi$ resonance in the neighborhood of the W mass, then $F_\pi(m_W^2)$ brings about an enhancement of W production. However, this enhancement is cancelled by the branching ratio of the W into all but the $\pi\pi$ decay modes. On the other hand $F_\pi(m_W^2)$ might be much less than one and would suppress the cross section below the values presented here. This suppression would not be compensated by the branching ratio.

One may also consider the lower vertex in Fig. 1 and look for an enhancement of the cross section that would come about by considering all inelastic final states for the target proton. (See the paper of H. Überall mentioned in Ref. 3.) Here again the enhancement is probably only of academic interest. In picking W events out of a large background it is unlikely that one could afford to throw away the kinematical information that a measurement of the recoil proton in $\pi^- + p \rightarrow W + p$ would give.

If there is any hope at all of detecting the W in the reaction considered here, it would appear to be via the $W^- \rightarrow \mu^-\bar{\nu}$ decay mode. The characteristic signature for this would be μ^-'s in the final state with large transverse momenta in the center-of-mass system. Such μ^-'s are possible because of the large Q value for the $\mu^-\bar{\nu}$ mode when m_W is in the multi-BeV

region. Using the helicity amplitudes presented in Section IV one can readily calculate the W density matrix and from it the angular distribution of the decay μ's.

ACKNOWLEDGEMENT

The author wishes to thank Professor S. D. Drell for suggesting this calculation and also Professor M. Jacob, Professor T. Truong and Dr. M. Bander for discussions concerning the absorption model. He also thanks S. Howry for assistance in using the Stanford B5500 computer.

REFERENCES

1. T. D. Lee and C. N. Yang, Phys. Rev. 119, 1410 (1960).
2. G. Bernardini, Rapporteur's talk 1964 International Conference of High-Energy Physics, Dubna (unpublished).
3. J. Bernstein and G. Feinberg, Phys. Rev. 125, 1741 (1962). Cross sections and decay angular distributions, without absorption, have been calculated for $m_W = 1.3\ m_N$ using this model by H. Uberall, Nucl. Phys. 58, 625 (1964).
4. R. P. Feynman and M. Gell-Mann, Phys. Rev. 109, 193 (1958).
5. We are making the usual assumption that the hadron weak currents transform under G according to: $GV_\alpha^H G^{-1} = +V_\alpha$ and $GA_\alpha G = -A_\alpha$ so that no "second class" terms are present in their matrix elements.
6. J. Bernstein, S. Fubini, M. Gell-Mann and W. Thirring, Nuovo Cimento 17, 757 (1960).
7. M. L. Goldberger and S. B. Treiman, Phys. Rev. 110, 1178 (1958).
8. M. A. Beg, J. M. Cornwall and C. H. Woo, Phys. Rev. Letters 12, 305 (1964).
9. K. Gottfried and J. D. Jackson, Nuovo Cimento 34, 735 (1964).
10. J. Donohue, K. Gottfried, R. Keyser and B. Suensson, Phys. Rev. 139, B428 (1965); J. D. Jackson, Rev. Mod. Phys. 37, 415 (1962); L. Durand and Y. Chiu, Phys. Rev. Letters 12, 399 (1964); Phys. Rev. 137, B1530 (1965).
11. Recent experiments [K. J. Foley, et al., Phys. Rev. Letters, 14, 862 (1965)] have shown that the forward $\pi^- p$ elastic scattering amplitudes have a non-zero real part that persists to the highest energies measured. The consequences of this real part for absorption model corrections remain, however, undiscussed.

12. K. J. Foley, et al., Phys. Rev. Letters 15, 45 (1965); 11, 425 (1963); S. Brandt, et al., Phys. Rev. Letters 10, 413 (1963).

13. See tabulation of C. Hohlen, C. Ebel and J. Giesecke, Z. Physik 180, 430 (1964).

14. M. Jacob and G. C. Wick, Ann. Phys. (N.Y.) 7, 404 (1959).

15. M. Bander and G. Shaw, Phys. Rev. 139, B956 (1965).

TABLE I

PION EXCHANGE TOTAL CROSS SECTIONS

W-MASS (BeV)	INCIDENT PION LAB ENERGY (BeV)	UNCORRECTED (10^{-34} cm^2)	CORRECTED FOR ABSORPTION	
			$\sigma_{tot}/4\pi A = 0.58$ (10^{-34} cm^2)	$\sigma_{tot}/4\pi = 1$ (10^{-34} cm^2)
2	6	210	60	9.3
2	8	200	44	12
2	10	180	33	12
2	12	170	25	10
2	14	160	20	8.8
2	16	150	16	7.3
3	12	260	54	7.8
3	14	250	47	10
3	16	240	42	11
3	18	220	38	12
4	18	310	55	5.5
4	20	300	51	7.0
4	22	290	49	8.4
4	24	280	46	9.6
5	26	350	53	4.5
5	28	340	52	5.6
5	30	340	51	6.7
5	32	330	50	7.7

TABLE II

RHO EXCHANGE TOTAL CROSS SECTIONS

W-MASS (BeV)	INCIDENT PION LAB ENERGY (BeV)	UNCORRECTED (10^{-34} cm^2)	CORRECTED FOR ABSORPTION	
			$\sigma_{tot}/4\pi A = 0.58$ (10^{-34} cm^2)	$\sigma_{tot}/4\pi = 1$ (10^{-34} cm^2)
2	8	4.6	2.0	0.11
2	10	5.5	2.5	0.17
2	14	6.6	3.0	0.26
4	18	2.4	0.86	0.023
4	22	3.6	1.4	0.066
4	26	4.5	1.8	0.11

LIST OF FIGURES

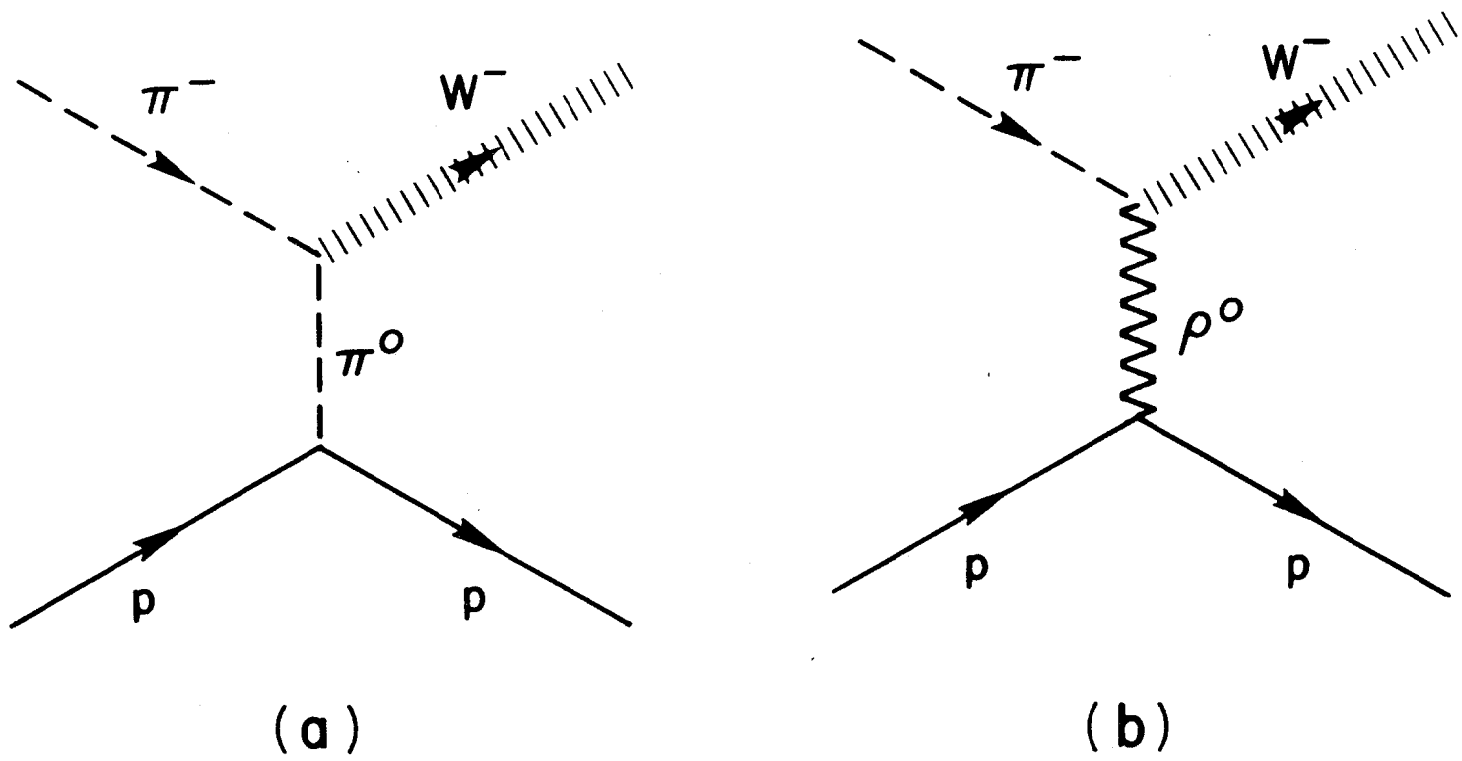

FIG. 1

428-1-A

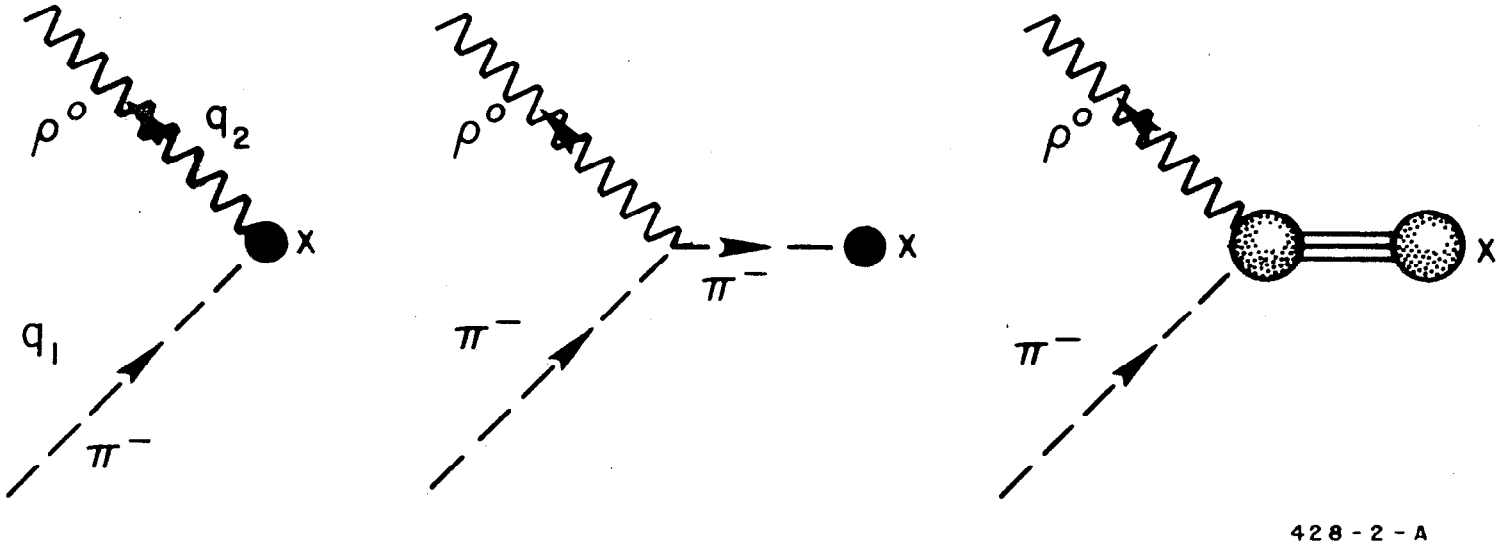

(a) (b) (c)

FIG. 2

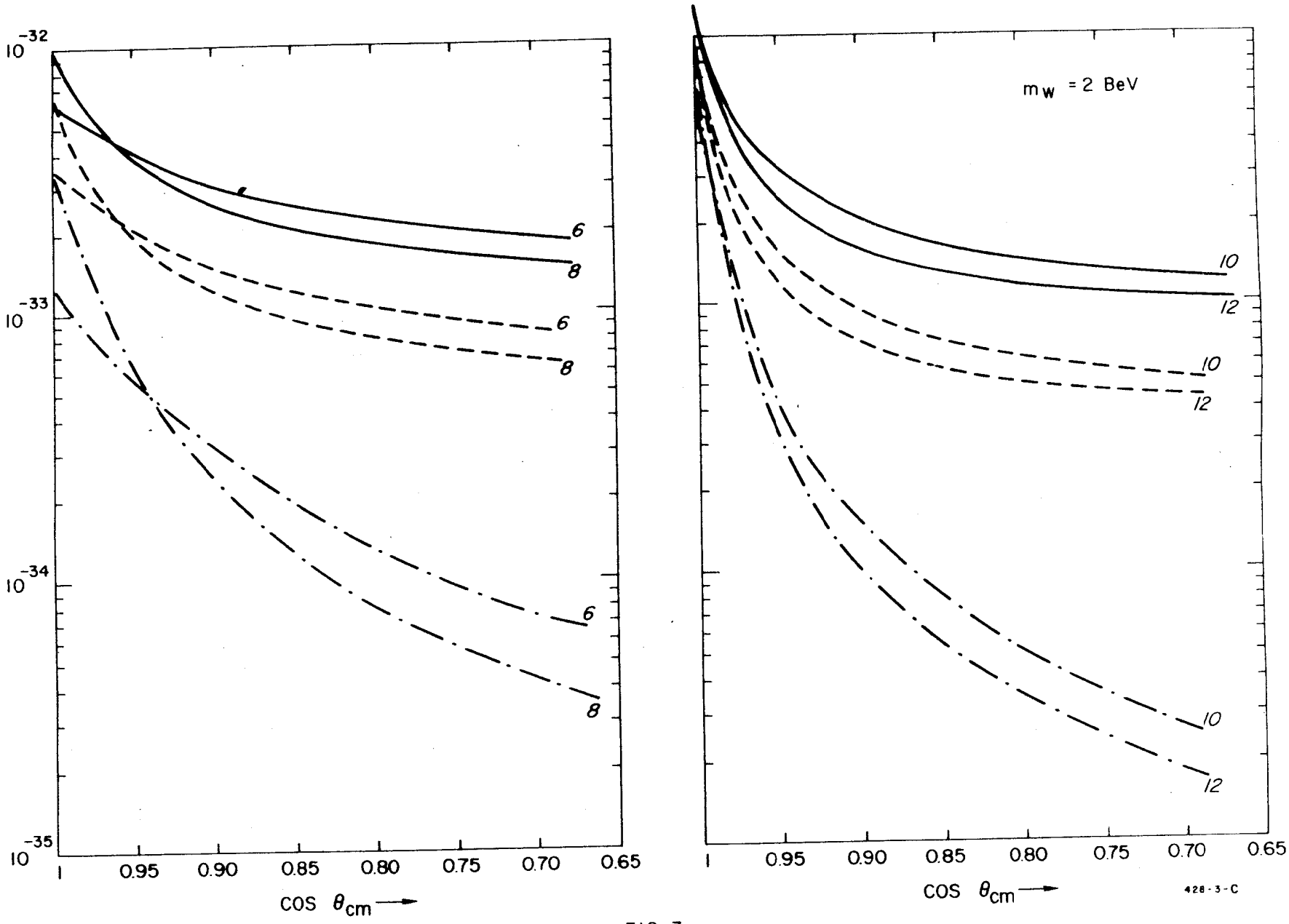
10^{-32}
10^{-33}
10^{-34}
10^{-35}
1
0.95
0.90
0.85
0.80
0.75
0.70
0.65
COS θ_{cm} →
6
8
6
8
6
8
m_W = 2 BeV
10
12
10
12
10
12
COS θ_{cm} →
428-3-C

FIG. 3

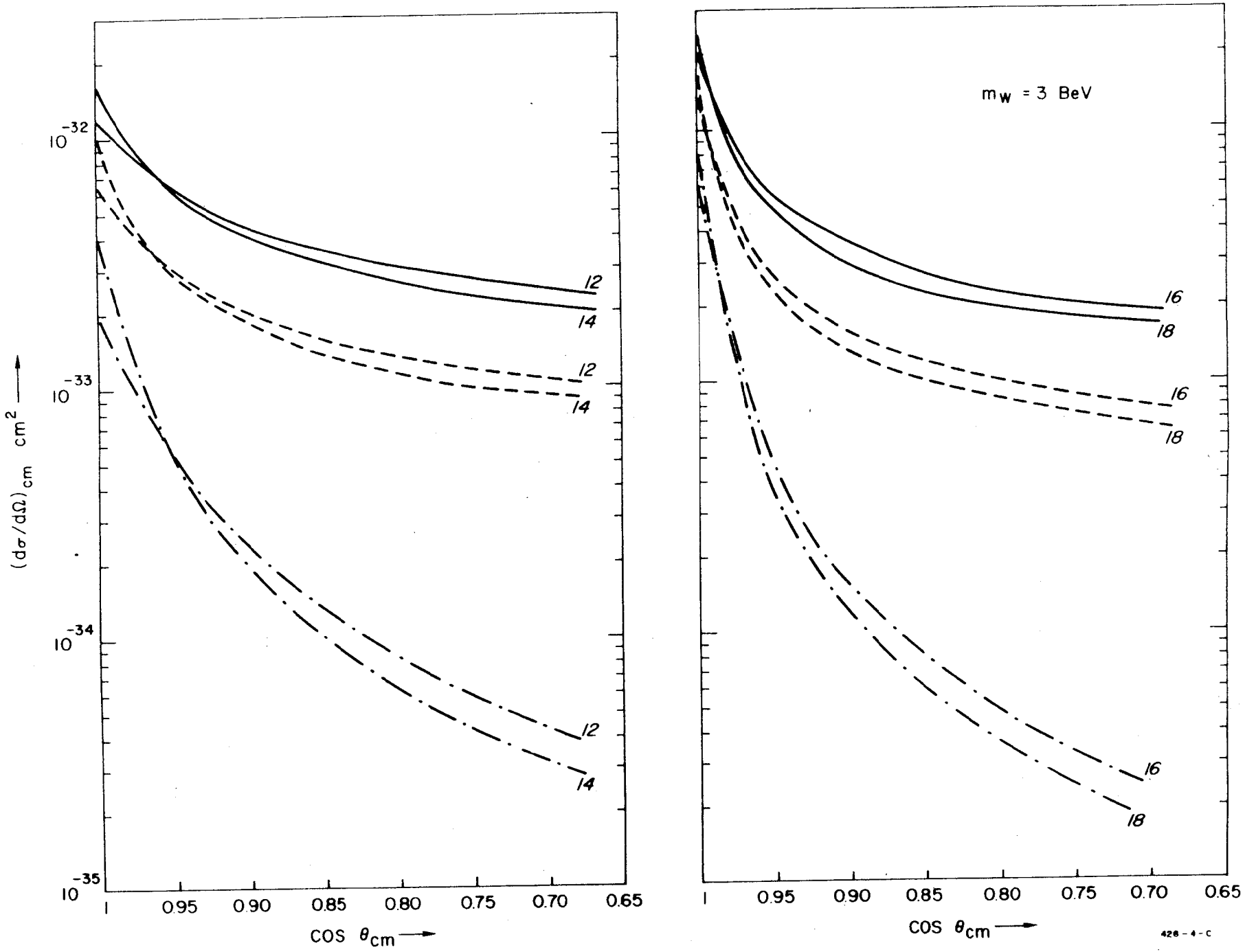
m_W = 3 BeV
$(d\sigma/d\Omega)_{cm}$ cm^2
10^{-32}
10^{-33}
10^{-34}
10^{-35}
12
14
12
14
12
14
16
18
16
18
16
18
1
0.95
0.90
0.85
0.80
0.75
0.70
0.65
COS θ_{cm}
426-4-C

FIG. 4

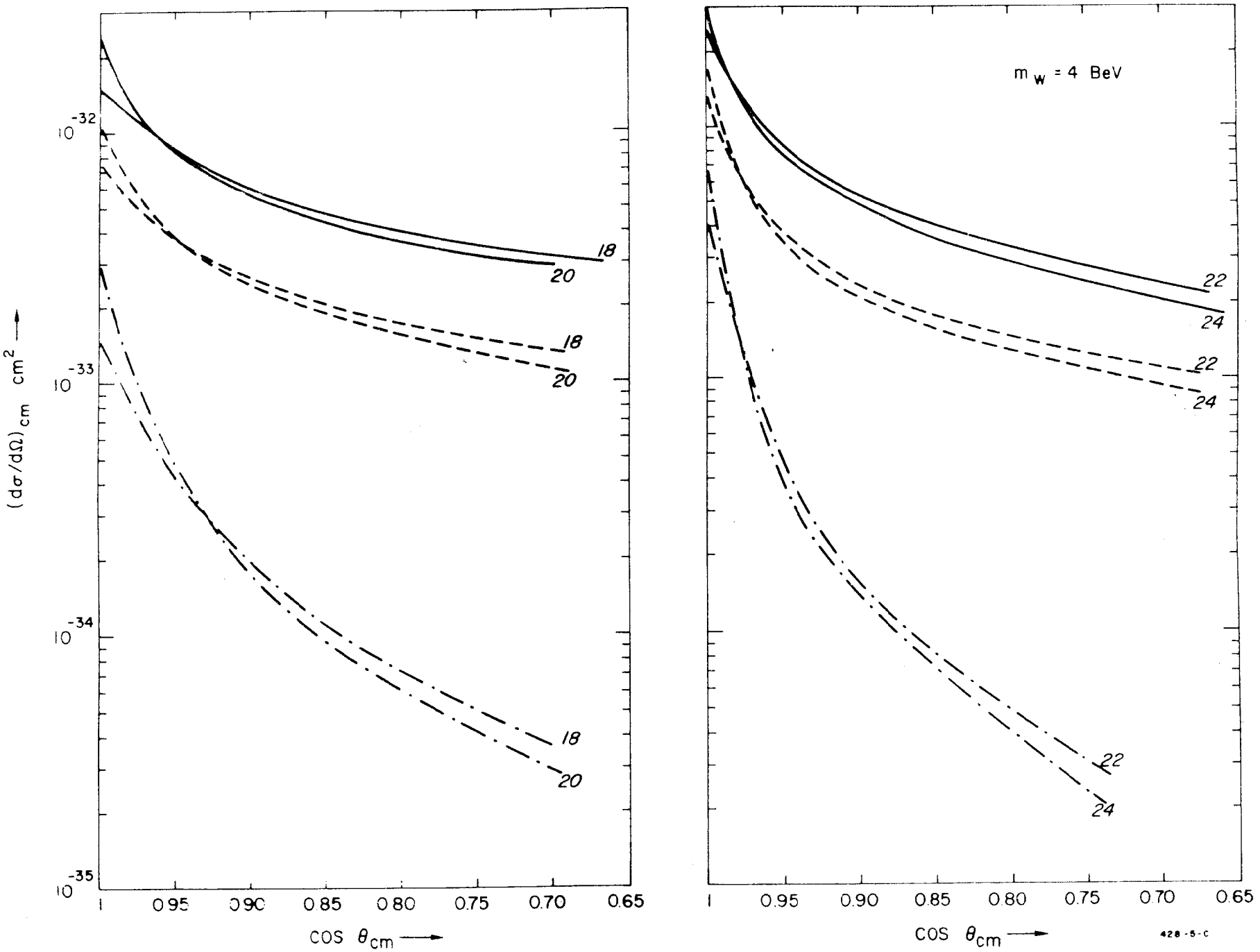
m_W = 4 BeV
$(d\sigma/d\Omega)_{cm}$ cm^2
10^{-32}
10^{-33}
10^{-34}
10^{-35}
18
20
18
20
18
20
22
24
22
24
22
24
1
0.95
0.90
0.85
0.80
0.75
0.70
0.65
cos θ_{cm}
cos θ_{cm}
428-5-C

FIG. 5

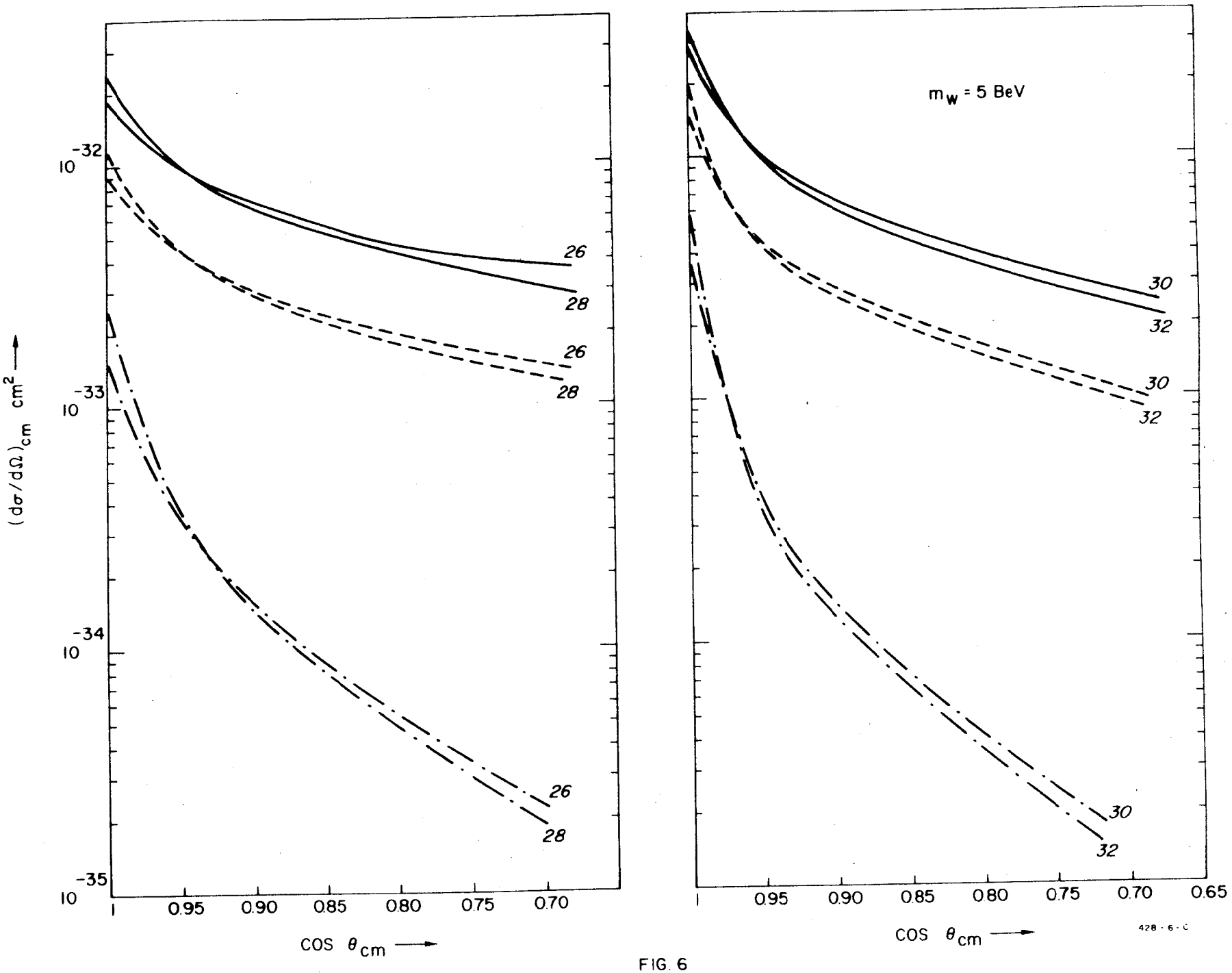
m_W = 5 BeV
$(d\sigma/d\Omega)_{cm}$ cm^2
10^{-32}
10^{-33}
10^{-34}
10^{-35}
26
28
26
28
26
28
30
32
30
32
30
32
1
0.95
0.90
0.85
0.80
0.75
0.70
0.65
COS θ_{cm}
COS θ_{cm}
428-6-C

FIG. 6

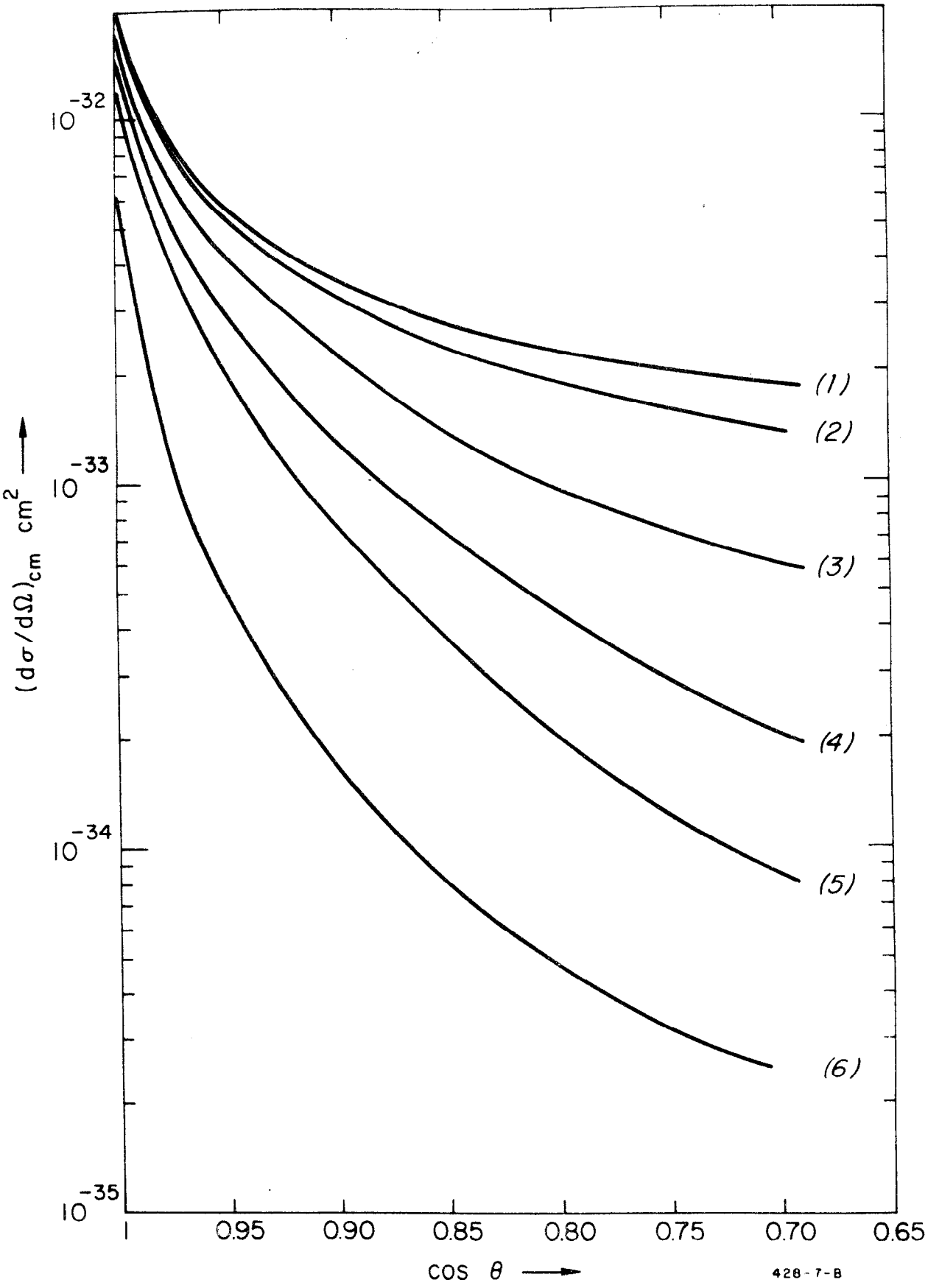
10^{-32}
10^{-33}
10^{-34}
10^{-35}
$(d\sigma/d\Omega)_{cm}$ cm^2
(1)
(2)
(3)
(4)
(5)
(6)
1
0.95
0.90
0.85
0.80
0.75
0.70
0.65
cos θ
428-7-B

FIG. 7

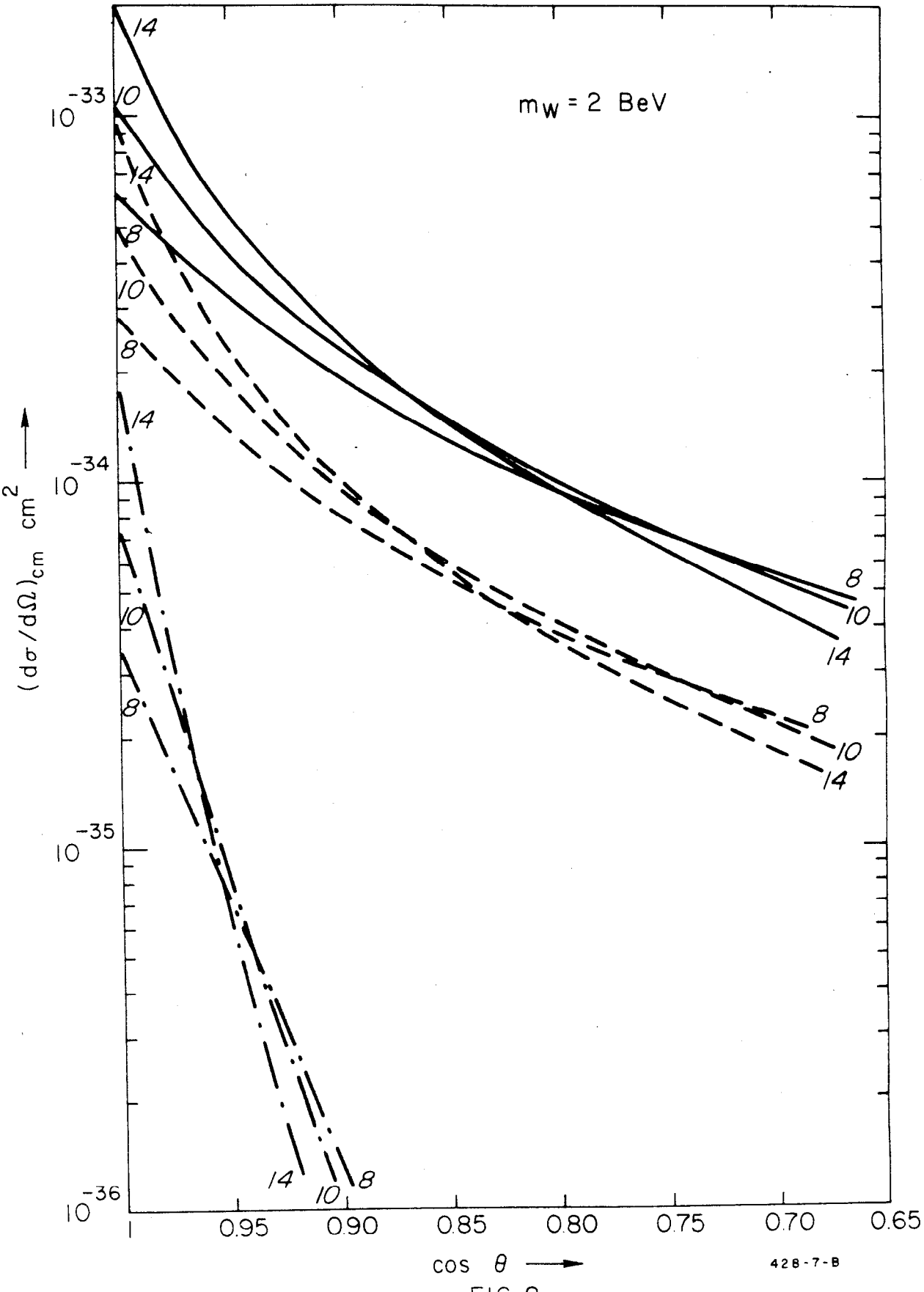
m_W = 2 BeV
10^{-33}
10^{-34}
10^{-35}
10^{-36}
$(d\sigma/d\Omega)_{cm}$ cm^2
1
0.95
0.90
0.85
0.80
0.75
0.70
0.65
cos θ
14
10
8
428-7-B

FIG. 8

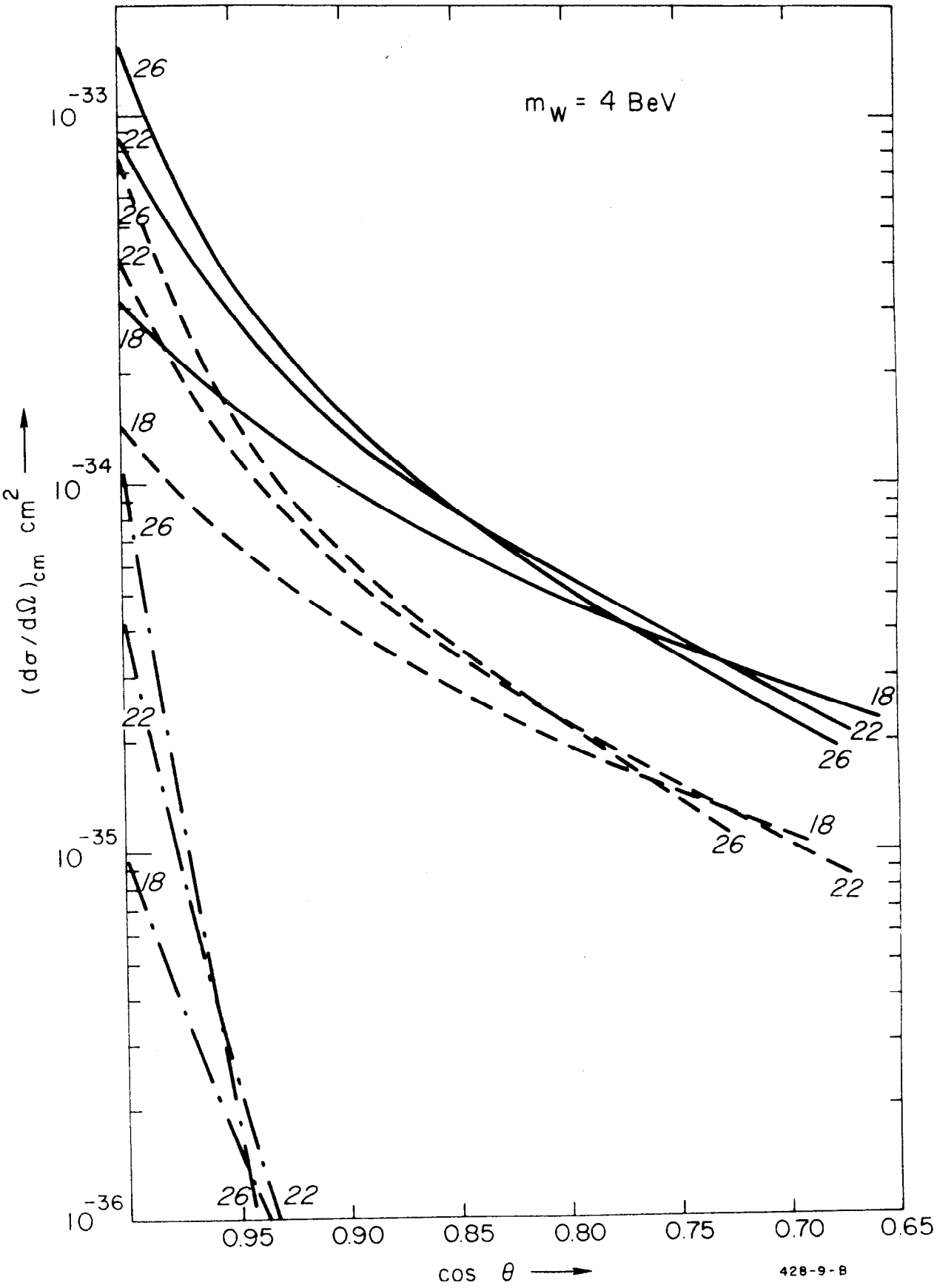
m_W = 4 BeV
$(d\sigma/d\Omega)_{cm}$ cm^2
10^{-33}
10^{-34}
10^{-35}
10^{-36}
26
22
18
0.95
0.90
0.85
0.80
0.75
0.70
0.65
cos θ
428-9-B

FIG. 9